Digital Manufacturing Technology
https://ojs.wiserpub.com/index.php/DMT/

UNIVERSAL WISER
PUBLISHER

Conference Proceeding

Paper presented at the 1st International Conference on Modern Technologies in Mechanical & Material Engineering [MTME 2023]

Enhanced Thermal Stability of Polymers by Incorporating Novel Surface-Decorated $SrTiO_3$@Graphene Nanoplatelets

Zia Ud Din, Mohsin Ali Marwat*, Amna Ijaz, Muhammad Ramzan Abdul Karim

Ghulam Ishaq Khan Institute of Engineering and Technology, Topi-23640, Swabi, Pakistan
E-mail: mohsin.ali@giki.edu.pk

Received: 25 May 2023; **Revised:** 11 July 2023; **Accepted:** 18 July 2023

Abstract: Polyvinylidene fluoride (PVDF) is a vital component in the manufacturing of flexible dielectric capacitors due to its exceptional electrical insulation properties. However, its thermal stability remains a significant concern. To address this, we have developed a novel approach in which surface-decorated $SrTiO_3$@Graphene (STO@G) nanoplatelets were prepared using a wet-chemical method. Subsequently, STO@G/PVDF nanocomposite films were synthesized via a solution-casting method using an automatic film coater. X-ray diffraction (XRD) analysis confirmed the presence of the required strontium titanate ($SrTiO_3$), graphene, and STO@G phases. Further, scanning electron microscopy (SEM) and energy-dispersive X-ray spectroscopy (EDXS) were used to examine the STO@G nanoplatelets' even distribution inside the PVDF polymer, even at higher nanoparticle concentrations (10 wt.%), revealing no porosity or morphological defects and demonstrating its potential for flexible dielectric capacitors. Thermogravimetric analysis (TGA) was used to assess the thermal stability of 10 wt.% STO@G/PVDF nanocomposite films, demonstrating a positive impact on PVDF's thermal stability. Specifically, the thermal stability of PVDF was enhanced until 170 ℃. These findings demonstrate that our approach provides a promising strategy to enhance the thermal stability of PVDF for various applications, including energy storage and conversion, sensors, and electronic devices, ultimately improving its reliability and durability by increasing its operational temperature range.

***Keywords*:** polymer nanocomposites, nanoparticles, thermal stability, surfaced-decorated nanoparticles

1. Introduction

Polymers have a diverse range of applications across multiple industries, such as packaging, construction, and electronics. However, their thermal stability is limited, which restricts their use in high-temperature applications [1-6]. Thus, there is a need to enhance the thermal stability of polymers for their wider utilization in various fields. One approach to achieving this is by incorporating nanoparticles that act as thermal barriers and reduce heat transfer to the polymer matrix [7]. Nanospheres, nanoplatelets, and nanocylinders offer several advantages, including enhanced thermal stability, greater stiffness, strength, and modulus. Researchers have used various polymers as the matrix phase, including linear polymers such as polyether imide (PEI), poly methyl methacrylate (PMMA), and poly ether sulfones (PES), as well as non-linear polymers based on polyvinylidene fluoride (PVDF) [3, 8, 9]. The nanofillers used in these materials include polyhedral oligomeric silsesquioxane (POSS), silica, alumina, titanium dioxide (TiO_2), clay, graphene,

DOI: https://doi.org/10.37256/dmt.3220233096

graphite, barium titanate ($BaTiO_3$), carbon nanotubes (CNTs), and strontium titanate ($SrTiO_3$), among others, which further enhance their properties [10].

Nanoparticles are to be dispersed uniformly in a polymer matrix which itself is a challenging task to have the desired and improved properties in polymer nanocomposites. To accomplish this, nanoparticles are probe-sonicated in the same solvent as that of the polymer and then added to the polymer slurry before being cast via a doctor blade to create a nanocomposite film [11]. The intermolecular interactions between nanoparticles and the polymeric film play a key in the behavior of the polymer chain's moment at the nanoparticle and matrix interface. These interactions can be either attractive or repulsive [12]. Therefore, enhancing the thermal properties of polymer-based nanocomposites requires an appropriate methodology to surface decorate nanofillers and modify the interfacial polymer layer properties [13]. Achieving the appropriate surface decoration of nanoparticles and modifying the properties of the interfacial polymer layer necessitates careful consideration of the method used. As a result, the resulting polymer nanocomposites can have significantly improved properties, including enhanced thermal stability, greater stiffness, strength, and modulus [14].

Thermal behavior is an essential area of interest in polymer nanocomposite research. Various properties of materials, including glass transition temperature, heat distortion temperature, and thermal expansion coefficient, can be measured through standard materials characterization techniques like thermogravimetric analyzer and thermomechanical analysis [2]. To check the thermal behavior of polymer-based nanocomposites One such characterization technique, thermogravimetric analysis (TGA), has been used most often [7]. TGA measures the loss in weight of the material while keeping a controlled atmosphere and varying temperature, providing important information regarding whether the material is thermally stable or not, such as degradation temperature and thermal decomposition rate [8]. The technique has been used to check out how the nanoparticles and their loading affect the thermal stability of the nanocomposites, providing a deeper understanding of the thermomechanical behavior of polymer nanocomposites [15-17].

In this study, a novel approach was developed to prepare surface-decorated $SrTiO_3$@Graphene (STO@G) nanoplatelets using a wet-chemical method. A subsequent step involved the synthesis of STO@G/PVDF nanocomposite films via the solution-cast method using an automatic film coater. The distribution of STO@G nanoplatelets within the PVDF polymer was investigated by scanning electron microscopy (SEM) and energy-dispersive X-ray spectroscopy (EDXS) and was found to be even at higher nanoparticle concentrations (10 wt.%), with no porosity or morphological defects. This result highlights the nanocomposite's potential for flexible dielectric capacitors. Furthermore, TGA was used for the evaluation of the thermal stability of 10 wt.% STO@G/PVDF nanocomposite films, demonstrating an enhancing impact on the thermal stability of PVDF. Specifically, the thermal stability of PVDF was enhanced until 170 ℃.

2. Experiment and methods

2.1 *Chemicals and materials*

Deionized water (DI water) was used as laboratory standard, N-methyl-2-pyrrolidone (NMP), PVDF, ethanol (99.9%), and graphene nanoplatelets (GNPs) and $SrTiO_3$ were obtained from Sigma Aldrich and used as procured.

2.2 *Synthesis of surface-decorated STO@G nanoparticles*

The present study involved the synthesis of surface-decorated STO@G nanoparticles by employing two different nanoparticles, namely, GNPs and $SrTiO_3$. The synthesis process involved the preparation of two separate solutions using stoichiometric ratios of 1:3 for GNPs and $SrTiO_3$. The reason for choosing this ratio is that it restrains from aggregation, i.e., $SrTiO_3$ nanoparticles act as spacers between GNPs nanoparticles, as a result, surface properties will be enhanced. For solution 1, 0.15 g of GNPs and 50% concentration of DI water and absolute ethanol (with purity greater than 99%) were mixed in a beaker having DI water and absolute ethanol 30 ml each. Solution 2 had the same concentration of DI water and ethanol as solution 1, but it contained 0.45 g of $SrTiO_3$. Both solutions were probe sonicated for 30 minutes to achieve uniform dispersion of particles, followed by stirring at 80 ℃ at 400 rpm for 2 hours. After stirring for 2 hours, solution 1 was added dropwise into solution 2 (containing $SrTiO_3$) while stirring for 3 hours at 80 ℃. The obtained STO@G nanoparticles were then dried in a vacuum oven for 8 hours. The STO@G nanoparticles were removed from the beaker, weighed (0.55 g), and preserved in a Petri dish.

2.3 *Synthesis of polymer film*

In this study, the synthesis of a polymer film involved the preparation of a slurry using PVDF powder and NMP solvent. Specifically, 0.5 g of PVDF powder was added to 5 g of NMP solvent at room temperature. A reason for choosing the 1:10 PVDF to NMP ratio is that it maintains the required amount of viscosity for making uniform and thin polymer films; the mixture was stirred constantly at 400 rpm for 2 hours to achieve homogeneity, as depicted in Figure 1(a).

The resulting solution had high viscosity, and a polymer film was obtained through tape casting on a glass substrate using an automatic film coater keeping the casting speed at 120 mm/min and set thickness at 0.75 mm, as shown in Figure 1(b) to achieve film thickness of 0.5 mm. The tape-cast film was subsequently dried for 3 hours at 80 ℃ in a vacuum oven, followed by the extraction of the film using ethanol, as shown in Figure 1(c).

Figure 1. (a) Synthesis of PVDF solution; (b) automatic film coater equipment is used for the solution casting of the flexible polymer film; (c) as-synthesized PVDF film over a glass substrate

2.4 *Synthesis of nanocomposite film*

In the subsequent stage of the experiment, a slurry of PVDF and NMP was prepared. Specifically, 1 g of PVDF was dissolved in 10 g of NMP, the solvent, and stirred for 2 hours at 80 ℃. For nanocomposite synthesis, 10 wt.% STO@G nanoparticles, i.e., 0.1 g for 1 g of PVDF were taken and mixed with 5 g of NMP, which was then subjected to probe sonication for 10 minutes. A reason for choosing such a ratio is that it maintains a compact, uniform, and viscous solution without any inconsistency and air bubbles, the mandatory aspects for a standard nanocomposite film. The resulting solution was added to the PVDF-NMP solution using a dropper while stirring at room temperature. The stirring was continued for 12 to 13 hours. The final step involved tape casting a composite film, which had the same thickness as the polymer film (0.5 mm). The film was cast onto a glass substrate using a doctor's blade. Due to concerns regarding film breakage, vacuum drying was deemed unsuitable. Instead, the film was dried for one hour without vacuum, followed by an additional hour of vacuum drying at 80 ℃, resulting in the formation of a composite film. Finally, the film was extracted using ethanol and preserved in an envelope for further analysis.

Figure 2. (a) Synthesis of STO@G/PVDF nanocomposite solution; (b) as-synthesized STO@G/PVDF nanocomposite film on a glass substrate

2.5 *Characterization*

In this study, the microscopic morphologies of the nanocomposite and STO@G were studied using SEM coupled with EDXS on a ZEISS instrument from the United Kingdom. The elemental structure identification of nanoparticles was carried out using X-ray diffraction (XRD) from Aporto, UK. To evaluate the thermal stability of the samples, a TGA from Perkin Elmer (STA 800, USA) was used.

3. Results and discussion

The results section represents the core findings of a study derived from the methods used to collect and analyze information. It presents these findings in a logical order without author bias or interpretation, preparing readers for subsequent interpretation and evaluation in the discussion section.

3.1 *XRD analysis*

The current investigation centered on the XRD analysis of GNPs, $SrTiO_3$, and surface-decorated STO@G nanoparticles. The confirmation of the presence of GNPs, $SrTiO_3$, and STO@G was performed by analyzing the peaks observed in Figure 3. The peaks obtained from the XRD analysis of GNPs and $SrTiO_3$ were compared with the literature values, which showed the presence of GNPs at (002) and multiple peaks at various 2θ angles that confirmed the presence of $SrTiO_3$ [18, 19]. Subsequently, the XRD analysis of STO@G was conducted. The obtained peaks matched with those of both GNPs and $SrTiO_3$, confirming the successful formation of surface-decorated nanoparticles.

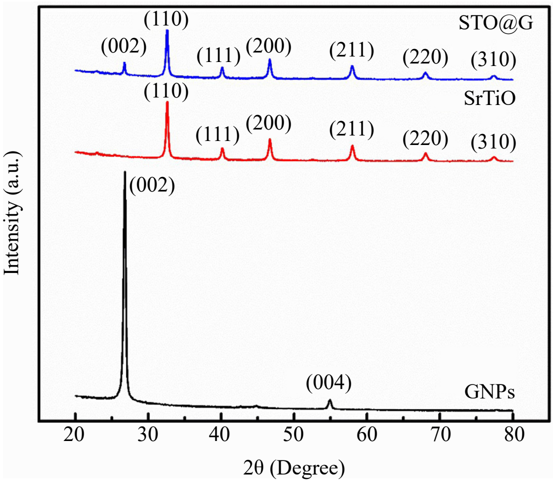

Figure 3. XRD graph of GNPs (black), $SrTiO_3$ (red), and STO@G (blue) nanoparticles

3.2 *SEM and EDXS analysis of STO@G nanoparticles*

The powder nanoparticles of STO@G were analyzed using SEM, and the obtained image is shown in Figure 4. The SEM analysis in Figure 4 illustrates the presence of white nanoparticles of $SrTiO_3$ clusters on black GNPs, indicating that the preparation of STO@G nanoparticles has been satisfactory [3, 20-23]. The figure shows the presence of white particles of $SrTiO_3$ clusters on black GNPs, suggesting that our preparation of STO@G nanoparticles has been satisfactory, and the $SrTiO_3$ nanoparticles adhere to the surface of GNPs. The greenish-dotted area indicates the GNPs while the yellowish-dotted area indicates white $SrTiO_3$ nanoparticles decorated onto the surface of GNPs.

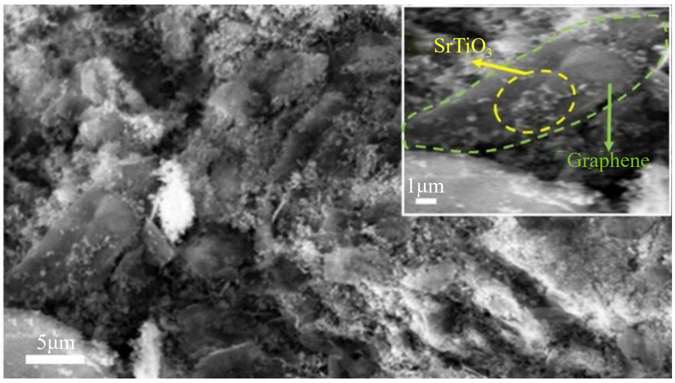

Figure 4. SEM image of STO@G nanoparticle

EDXS is an elemental analysis EDXS graph between the energy of characteristics X-rays and intensity or counts. Figure 5 illustrates the EDXS of STO@G, which confirms the presence of constituent elements and their relative counts to each other. As we know we took the ratio of $SrTiO_3$ and GNPs as 3:1, so Sr will have higher intensity than carbon and oxygen shows the powder is made of GNPs and $SrTiO_3$.

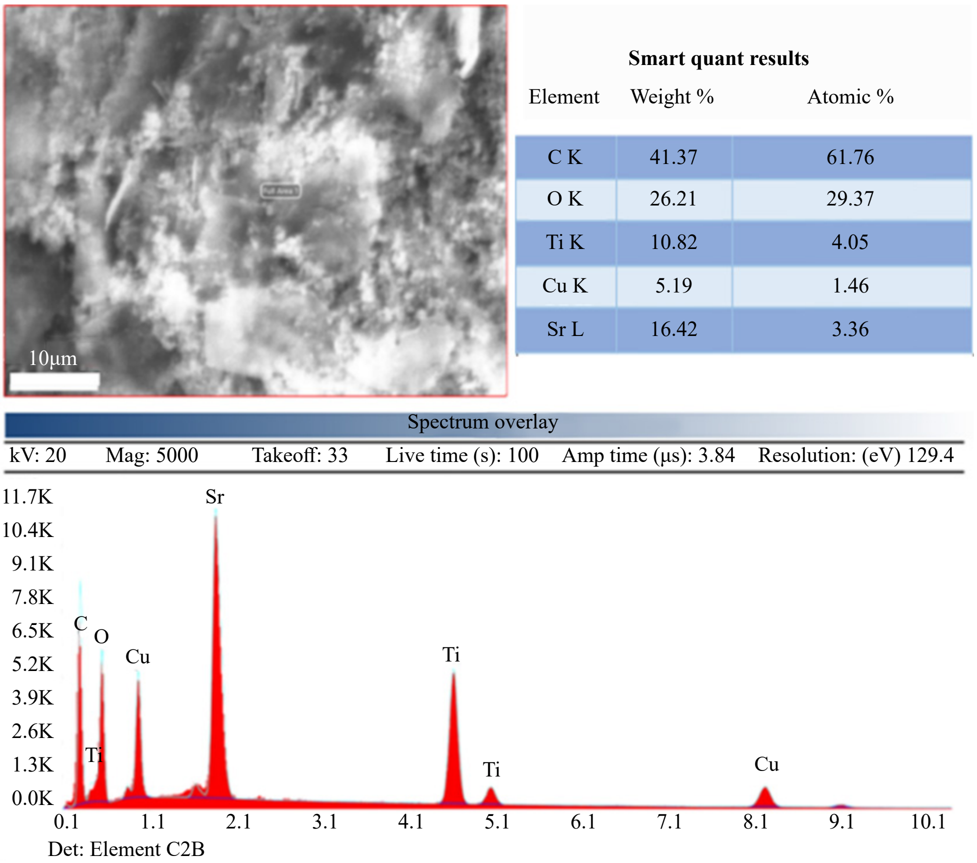

Smart quant results

Element	Weight %	Atomic %
C K	41.37	61.76
O K	26.21	29.37
Ti K	10.82	4.05
Cu K	5.19	1.46
Sr L	16.42	3.36

kV: 20 Mag: 5000 Takeoff: 33 Live time (s): 100 Amp time (µs): 3.84 Resolution: (eV) 129.4

Det: Element C2B

Figure 5. EDXS results of STO@G nanoparticles

3.3 *SEM and EDXS analysis of nanocomposite film*

The micrograph of the nanocomposite film presented in Figure 6 confirms the presence of STO@G nanoparticles in the PVDF matrix. The image displays white STO@G nanoparticles in the black PVDF matrix and their dispersion is uniform throughout the matrix. This confirms the successful incorporation of the nanoparticles into the polymer matrix, which can be further analyzed for various applications.

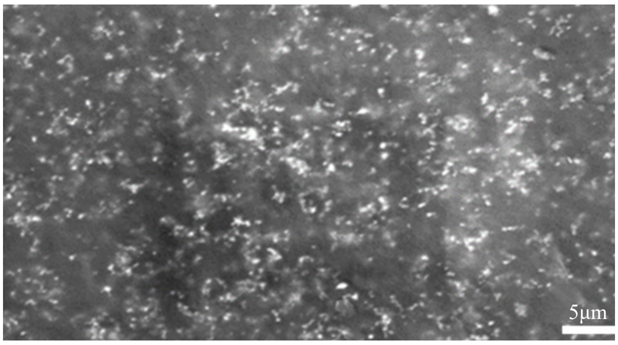

Figure 6. SEM image of STO@G/PVDF nanocomposite films

The EDXS analysis of the nanocomposite film confirms the presence of PVDF and STO@G. Figure 7 displays different peaks obtained from the analysis. As it is clear that STO@G/PVDF film has a high concentration of PVDF, the intense curve of high counts at the excitation voltage of carbon and fluorene shows the presence of PVDF. Additionally, the presence of oxygen and strontium confirms the presence of graphene oxide and $SrTiO_3$ nanoparticles.

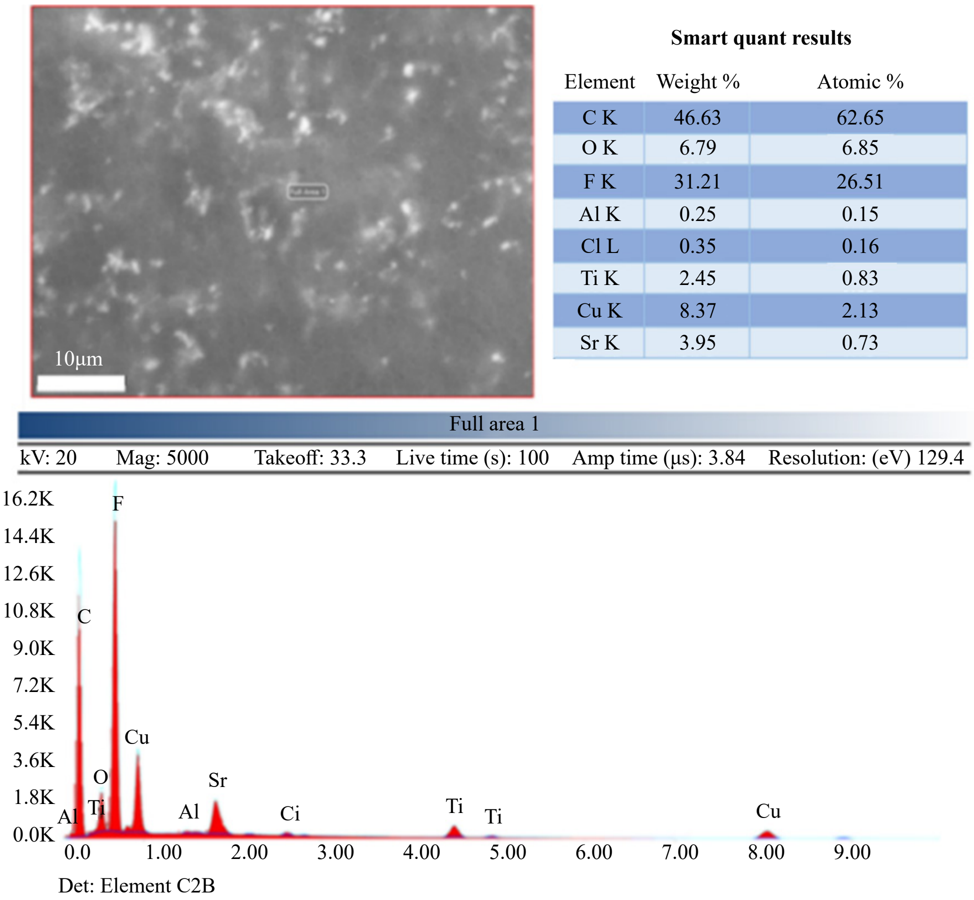

Smart quant results

Element	Weight %	Atomic %
C K	46.63	62.65
O K	6.79	6.85
F K	31.21	26.51
Al K	0.25	0.15
Cl L	0.35	0.16
Ti K	2.45	0.83
Cu K	8.37	2.13
Sr K	3.95	0.73

Figure 7. EDXS results of STO@G/PVDF nanocomposites

3.4 *TGA analysis*

The thermal properties of both the nanocomposite and polymer films were assessed by employing TGA using nitrogen atmosphere, at 10 ℃/min as the heating rate. Figure 8 depicts the thermogram displaying the thermal decomposition of both PVDF and PVDF nanocomposite film. The experimental data indicate that PVDF and STO@G/PVDF nanocomposite exhibit dissimilar thermal behavior. To improve the thermal stability, STO@G nanoparticles with surface decoration were utilized, resulting in an enhancement in the thermal stability of PVDF. The TGA curves of both PVDF and the STO@G/PVDF nanocomposite reveal that the incorporation of nanoparticles led to enhanced thermal stability as the starting temperature of degradation for the nanocomposite was higher than the PVDF polymer, demonstrating less weight loss and increased thermal stability until 170 ℃. This is due to the high thermal stability of $SrTiO_3$, which acts as a thermal barrier, thereby reducing the transfer of heat to the polymer matrix, and ultimately increasing thermal stability. The nanocomposite displays a decrease in thermal stability between 200 ℃ to 480 ℃ due to the presence of GNPs, which are less thermally stable than PVDF. However, at higher temperatures, the nanocomposite exhibits greater thermal stability due to the aforementioned role of nanoparticles as a thermal barrier. At 500 ℃, the nanocomposite experiences a 52% weight loss, whereas PVDF undergoes a 70% weight loss. Similarly, at 800 ℃, the nanocomposite exhibits a 68% weight loss, while PVDF experiences an 82% weight loss. Overall, the TGA analysis indicates that the thermal stability of PVDF is enhanced by the incorporation of surface-decorated STO@G nanoparticles.

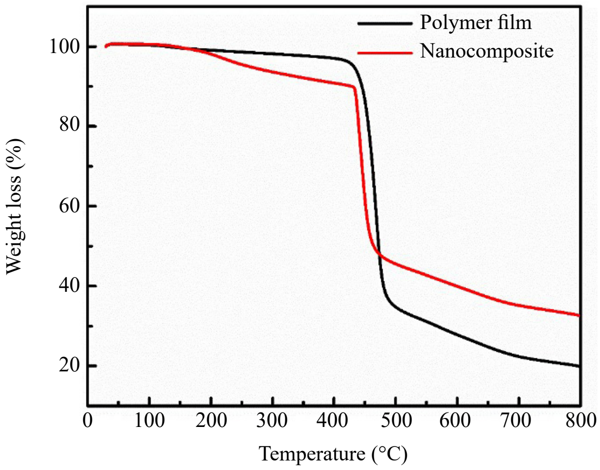

Figure 8. TGA graph of PVDF (black line) and STO@G polymer nanocomposite (red line) films

4. Conclusions

In conclusion, our research has successfully demonstrated a novel approach to enhance the thermal stability of PVDF using surface-decorated STO@G. We prepared STO@G using a wet-chemical method and synthesized STO@G/PVDF nanocomposite films via an automatic film coater using a solution cast method. Our findings from XRD analysis have ensured the presence of the required $SrTiO_3$, graphene, and STO@G phases. SEM and EDXS showed that the STO@G nanoplatelets were evenly distributed inside the PVDF polymer, even at higher nanoparticle concentrations (10 wt.%), without any porosity or morphological defects, indicating its potential for flexible dielectric capacitors. Furthermore, our TGA results demonstrated a positive impact of STO@G on PVDF's thermal stability. Therefore, our approach provides a promising strategy to enhance the thermal stability of PVDF for various applications, including energy storage and conversion, sensors, and electronic devices, ultimately improving its reliability and durability by increasing its operational temperature range. These findings contribute to the development of more efficient and robust materials for diverse applications in various industries.

Acknowledgments

The authors acknowledge the Higher Education Commission (HEC) of Pakistan because the thermal analysis has been performed on STA-8000 (Perkin Elmer USA) obtained from the generous funding provided by HEC via project # NRPU 10493.

Conflict of interest

There is no conflict of interest for this study.

References

[1] Ouyang ZW, Chen EC, Wu TM. Thermal stability and magnetic properties of polyvinylidene fluoride/magnetite nanocomposites. *Materials*. 2015; 8(7): 4553-4564. https://doi.org/10.3390/ma8074553

[2] Begum S, Ullah H, Ahmed I, Zhan Y, Kausar A, Aleem MA, et al. Investigation of morphology, crystallinity, thermal stability, piezoelectricity and conductivity of PVDF nanocomposites reinforced with epoxy functionalized MWCNTs. *Composites Science and Technology*. 2021; 211: 108841. https://doi.org/10.1016/j.compscitech.2021.108841

[3] Marwat MA, Yasar M, Ma W, Fan P, Liu K, Lu D, et al. Significant energy density of discharge and charge-discharge efficiency in Ag@BNN nanofillers-modified heterogeneous sandwich structure nanocomposites. *ACS Applied Energy Materials*. 2020; 3(7): 6591-6601. https://doi.org/10.1021/acsaem.0c00770

[4] Marwat MA, Xie B, Zhu Y, Fan P, Ma W, Liu H, et al. Largely enhanced discharge energy density in linear polymer nanocomposites by designing a sandwich structure. *Composites Part A: Applied Science and Manufacturing*. 2019; 121: 115-122. https://doi.org/10.1016/j.compositesa.2019.03.016

[5] Marwat MA, Xie B, Zhu Y, Fan P, Liu K, Shen M, et al. Sandwich structure-assisted significantly improved discharge energy density in linear polymer nanocomposites with high thermal stability. *Colloids and Surfaces A: Physicochemical and Engineering Aspects*. 2019; 581: 123802. https://doi.org/10.1016/j.colsurfa.2019.123802

[6] Marwat MA, Xie B, Ashtar M, Zhu Y, Fan P, Zhang H. High remnant polarization, high dielectric constant and impedance performance of Nb/In Co-doped $Bi_{0.49}La_{0.01}Na_{0.49}Li_{0.01}TiO_{3-\delta}$ ceramics. *Ceramics International*. 2018; 44(6): 6843-6850. https://doi.org/10.1016/j.ceramint.2018.01.108

[7] Marwat MA, Ma W, Fan P, Elahi H, Samart C, Nan B, et al. Ultrahigh energy density and thermal stability in sandwich-structured nanocomposites with dopamine@Ag@$BaTiO_3$. *Energy Storage Materials*. 2020; 31: 492-504. https://doi.org/10.1016/j.ensm.2020.06.030

[8] Ahmed N, Khan ZS, Ashraf A, Pervaiz H, Marwat MA, Qayyum AA. Si diffusion induced adhesion and corrosion resistance in annealed RF sputtered SiC films on graphite substrate. *Ceramics International*. 2022; 48(8): 11009-11017. https://doi.org/10.1016/j.ceramint.2021.12.321

[9] Marwat MA, Xie B, Zhu Y, Fan P, Ashtar M, Zhang H. Trilayered barium titanate/poly(methyl methacrylate) nanocomposites with enhanced breakdown strength and energy density. In: *The 10th China-Japan Symposium on Ferroelectric Materials and Their Applications (JCFMA-10)*. Inuyama, Japan: JCFMA-10; 2018. https://www.researchgate.net/publication/343513603

[10] Zhu Y, Yuan S, Lu C, Xie B, Fan P, Marwat MA, et al. High discharged energy density of nanocomposites filled with double-layered core-shell nanoparticles by reducing space charge polarization. *Ceramics International*. 2018; 44(16): 19330-19337. https://doi.org/10.1016/j.ceramint.2018.07.161

[11] Liu K, Marwat MA, Ma W, Wei T, Li M, Fan P, et al. Enhanced energy storage performance of nanocomposites filled with paraelectric ceramic nanoparticles by weakening the electric field distortion. *Ceramics International*. 2020; 46(13): 21149-21155. https://doi.org/10.1016/j.ceramint.2020.05.192

[12] Nie RP, Lei J, Jia LC, Chen C, Xu L, Li Y, et al. Significantly improved high-temperature performance of polymer dielectric via building nanosheets and confined space. *Composites Part B: Engineering*. 2020; 196: 108108. https://doi.org/10.1016/j.compositesb.2020.108108

[13] Su Y, Li W, Yuan L, Chen C, Pan H, Xie G, et al. Piezoelectric fiber composites with polydopamine interfacial layer for self-powered wearable biomonitoring. *Nano Energy*. 2021; 89: 106321. https://doi.org/10.1016/j.nanoen.2021.106321

[14] Zhu J, Wang D, Liu Z, Leung CM, Chen J, Zeng M, et al. Superior energy storage of sandwiched PVDF films by separate introduction of core-shell Ag@BT nanoparticles and 2D MXene nanosheets. *Ceramics International*. 2022; 48(13): 19274-19282. https://doi.org/10.1016/j.ceramint.2022.03.220

[15] Fan P, Zhang Y, Zhu Y, Ma W, Liu K, He X, et al. Large strain under low driving field in lead-free relaxor/ferroelectric composite ceramics. *Journal of the American Ceramic Society*. 2019; 102(7): 4113-4126. https://doi.org/10.1111/jace.16256

[16] Khan MF, Marwat MA, Shah SS, Karim MRA, Aziz MA, Din ZU, et al. Novel MoS_2-sputtered NiCoMg MOFs for high-performance hybrid supercapacitor applications. *Separation and Purification Technology*. 2023; 310: 123101. https://doi.org/10.1016/j.seppur.2023.123101

[17] Ali S, Marwat MA, Khan MF, Adam KM, Din ZU, Karim MRA, et al. Ti_3SiC_2-coupled NiCoMn LDH nanocomposites as positive electrode for high performance supercapacitors. *Journal of Alloys and Compounds*. 2023; 956: 170229. https://doi.org/10.1016/j.jallcom.2023.170229

[18] Da Silva LF, Maia LQ, Bernardi MIB, Andrés JA, Mastelaro VR. An improved method for preparation of $SrTiO_3$ nanoparticles. *Materials Chemistry and Physics*. 2011; 125(1-2): 168-173. https://doi.org/10.1016/j.matchemphys.2010.09.001

[19] Alkhamis M, Imqam A. New cement formulations utilizing graphene nano platelets to improve cement properties and long-term reliability in oil wells. In: *SPE Kingdom of Saudi Arabia annual technical symposium and exhibition.* Dammam, Saudi Arabia: OnePetro; 2018. https://doi.org/10.2118/192342-MS

[20] Ashtar M, Marwat MA, Gao YX, Zhang ZT, Pi L, Yuan SL, et al. $REZnA_{11}O_{19}$ (RE = Pr, Nd, Sm–Tb): A new family of ideal 2D triangular lattice frustrated magnets. *Journal of Materials Chemistry C*. 2019; 7(32): 10073-10081. https://doi.org/10.1039/C9TC02643F

[21] Xie B, Zhang L, Marwat MA, Zhu Y, Ma W, Fan P, et al. High energy storage performance for dielectric film capacitors by designing 1D $SrTiO_3$@SiO_2 nanofillers. *Journal of Advanced Dielectrics*. 2018; 8(6): 1850039. https://doi.org/10.1142/S2010135X1850039X

[22] Marwat MA, Ullah H, Usman M, Ehsan MA, Zhang H, Khan MF, et al. Significantly improved photocatalytic activity of the $SnO_2/BiFeO_3$ heterojunction for pollutant degradation and mechanism. *Ceramics International*. 2022; 48(10): 14789-14798. https://doi.org/10.1016/j.ceramint.2022.02.016

[23] Ali S, Marwat MA, Khan MF, Adam KM, Din ZU, Karim MRA, et al. Ti_3SiC_2-coupled NiCoMn LDH nanocomposites as positive electrode for high performance supercapacitors. *Journal of Alloys and Compounds*. 2023; 956: 170229. https://doi.org/10.1016/j.jallcom.2023.170229